# Single and population coding of taste in the gustatory cortex of awake mice

David Levitan[2]*, Jian-You Lin[1,3]*, Joseph Wachutka[2], Narendra Mukherjee[2], Sacha B. Nelson[2,3,4], Donald B. Katz[1,3]

Departments of Psychology[1] and Biology[2], Volen Center for Complex Systems[3], National Center for Behavioral Genomics[4], Brandeis University, Waltham, Massachusetts 02454, USA.

**Abbreviated Title:** Taste Processing in Mouse Gustatory Cortex
**Number of Pages**: 37
**Figures:** 9
**Abstract:** 247
**Introduction**: 582
**Discussion:** 875

**Declaration of Interest:** The authors declare no competing financial interests.

**Acknowledgements:** This research was supported by the National Institute on Deafness and Other Communication Disorders (NIDCD) DC006666.

Proofs and correspondence to corresponding Author:

**Donald B Katz, PhD**
Brandeis University
Department of Psychology, MS 062
415 South Street
Waltham, MA 02454
Email: dbkatz@brandeis.edu

**Abstract**

A great deal is known about the broad coding and neural ensemble dynamics characterizing forebrain taste processing in awake rats, and about the relationship between these firing rate dynamics and behavior. With regard to mice, in contrast, data concerning cortical taste coding are few, inconclusive, and largely restricted to imaging, which lacks the temporal sensitivity necessary for evaluation of fast response dynamics. Here we have recorded the spiking activity of ensembles of gustatory cortical (GC) single neurons while presenting representatives of the basic taste modalities (sweet, salty, sour and bitter) to awake mice. Our results reveal deep similarities between rat and mouse taste processing. Many recorded murine GC neurons (~66%) responded distinctly to different tastes, and entropy analysis (which measures the breadth of taste coding) further confirmed that the majority of taste neurons in fact responded to 3 or 4 tastes. Temporal coding analyses revealed that single mouse GC neurons sequentially coded taste identity and palatability—the latter responses emerging ~0.5s after the former—a dynamic that population analysis suggested reflects a reliable sequence of network states activated by taste delivery (i.e., ensembles of simultaneously-recorded neurons transitioned suddenly and coherently from coding taste identity to coding taste palatability). All of the above results held across the anterior-posterior and dorsal-ventral axes of GC—neither between- nor within-mouse mapping revealed regions of narrow or temporally simple taste responses. In conclusion, our data indicates that mouse GC, like rat GC, codes multiple aspects of taste in a coarse, time-varying manner.

## Introduction

Mice are currently the most commonly used subjects in vertebrate neuroscience research; the decision to use mice affords researchers improved access to the molecular and genetic underpinnings of network activity, learning-related plasticity, and behavior (Stevens, 1996; Kandel et al., 2014; Trouche et al., 2016; Talbot et al., 2018). As taste is a particularly good sensory system with which to study these three topics (see below and Carleton et al., 2010; Maffei et al., 2012), it is surprising that relatively little work has been done on the electrophysiology of sensory responses within the taste neuroaxis in awake mice. In fact, there has been almost no extensive analysis of central taste electrophysiology in mice (although see Kusamoto-Yoshida et al., 2015): most *in vivo* assays of murine taste responses come from imaging work, the results of which have been difficult to reconcile with one another (Chen et al., 2011; Fletcher et al., 2017) and with related rat work (which consistently suggests broad responsiveness of regions and individual neurons, see Accolla et al., 2007; Jezzini et al., 2013; Sadacca et al., 2012; Samuelsen & Fontanini, 2017); in particular, it is difficult to analyze fast and subtle neural dynamics (see below) using imaging data.

In contrast, a good deal of coherent progress has been made toward characterizing primary gustatory cortical (GC) taste responses in awake rats, mainly (but not ubiquitously) using electrophysiology. This work has exposed reliable properties of taste spiking activity in relation to behavior, specifically revealing: 1) that single-neuron taste responses vary widely in breadth, with responses to multiple tastes appearing in the same region, and even within the same single neurons (Katz et al., 2001; Fontanini & Katz, 2006; Accolla et al., 2007; Samuelsen et al., 2013); 2) that these responses progress

through a series of firing-rate “epochs,” coding in turn the presence, physical properties, and palatability of a taste across 1-1.5s (Katz et al., 2001; Bahar et al., 2004; Sadacca et al., 2012; Maier & Katz, 2013; Samuelsen et al., 2013); 3) that the late-epoch palatability-related firing is uniquely affected by experience-driven shifts of taste palatability (Bahar et al., 2004; Fontanini & Katz, 2006; Grossman et al., 2008; Moran and Katz., 2014); and 4) that in single trials the onset of palatability is a sudden, coherent network phenomenon, the timing of which predicts and impacts behavior (Jones et al., 2007; Sadacca et al., 2016; Li et al., 2016). A test of whether mouse GC neurons respond in a like manner has not yet been performed.

In the current study we do precisely this, recording the responses of small ensembles of GC neurons (10-39 neurons/ensemble) in awake mice to presentations of stimuli representing four major taste modalities (sweet, salty, sour and bitter). Our data reveal that taste responses in murine GC recapitulate the basic principles of taste responses in rat GC: taste delivery evoked broad and dynamic responses which coded taste identity followed by taste palatability; Furthermore, these single-neuron dynamics reflected coherent ensemble transitions. We took care to map the spatial extent of GC, and were able to show all of these response properties to be distributed uniformly along the anterior-posterior and dorsal-ventral axes; we observed no regions of noticeably sparse responsiveness, and no regions in which responses failed to reflect the general dynamics. These results offer insight into mouse cortical taste processing—insight that can be used, in conjunction with tools available only in the mouse (among mammals), to delve into the undoubtedly rich relationship between molecular and network analyses of sensory function.

## Material and Methods

*Subjects*

The experimental subjects were C57BL/6J (n = 2) and Stk11tm1.1Sjm (StK11; n = 4) mice. The mice were purchased from Jackson Laboratories (Bar Harbor, ME). Stk11f/f mice have conditional floxed allele between exon 3 and exon 6, which was inactive through the entire set of experiments. Thess mice were backcrossed after development by the donating investigator for at least 4 generations to C57BL/6J mice and were inbreed to C57BL/6J for at least one generation in upon arrival to Jackson Laboratories (see also Nakada et al., 2010). After the mice were purchased from Jackson Laboratories they were further backcrossed for 3-4 generation to C57BL/6J before establishing a colony.

As no behavioral or neural taste response differences distinguished the strains, they are collapsed into a single group for purposes of our analyses. Upon arrival, the mice were placed on a 12-hour light-dark cycle, and given *ad libitum* access to food and water except during experimentation, at which time water access was restricted (see the session of "Taste array stimulation") while food remained available *ad libitum* (note that animals reliably consume less food when deprived of water). Experiment procedures started once mice were 60-80 days old. All procedures were approved by the Brandeis University Institutional Animal Care and Use Committee (IACUC) and in accord National Institutes of Health guidelines.

*Surgery*

Mice were anesthetized with an intraperitoneal (ip) injection of ketamine/xylazine mix (KX; 20mg/ml ketamine, 2.5 mg/ml Xylazine, and 0.5 mg/ml Aceptomazine; total injection

volume 5µl/g), and stabilized in a stereotaxic frame. A midline incision on the scalp exposed the skull, and 2 trephine holes were made dorsal to GC. Multi-channel electrodes (16 formvar-coated, 25 µm nichrome wires) were gradually lowered into the holes, to a spot just dorsal to GC (AP= 1.0 mm, ML= ±3 mm; DV= -2.25 mm). Electrode assemblies were then cemented to the skull, along with one intraoral cannula (IOC; flexible plastic tubing inserted in the cheek and extending upward to the top of the skull).

Mice were given 7 days to recover from the surgery. During the first 3 days of this recovery, injections of meloxicam (2 mg/kg), ip) and penicillin (0.1 ml), both administered subcutaneously, provided pain and infection management, respectively.

*Fluid delivery protocol*

For the three days following recovery from surgery, mice received one 30-min session per day in which 60 deliveries (hereafter, “trials”) of water were delivered. This procedure habituated the mice to the experimental environment, and to IOC delivery of fluid. Following delivery of the last session of water, the electrodes were lowered 200-250 µm and mice were returned to home cage.

On the day following the third adaptation day, the recording experiment started. The procedure was identical to that described above, except that water was replaced with 4 different taste stimuli, which were sweet—0.2 M sucrose, salty—0.1 M sodium-chloride, sour-0.02 M citric-acid and bitter-0.001 M quinine. Thus, 15 trials of each taste were delivered, in random order (sampling without replacement). These tastes and concentrations were chosen both to provide compatibility to our prior research and because they provided a broad range of both quality and palatability.

A subset of mice (N=4) received two identical recording sessions separated by one day. In these cases, the electrodes were lowered ~ 250 µm immediately after the first recording session. No substantive between-day differences were noted, and the data from the two were combined.

*Acquisition of electrophysiological data*

Voltage signals from the micro-electrodes were sampled at 30 kHz, digitally amplified and filtered, and saved to the hard drive of an Ubuntu computer connected to an Intan recording system (RHD2000 Evaluation System and Amplifier Boards; Intan Technologies, LLC, LA). From these raw voltage signals, we retained all waveforms and sorted the resulting waveforms into distinct units on the basis of S:N (>3:1) and distinctiveness of wave shape, using customized python scripts (for details see Mukherjee et al., 2017). A total of 185 single units were isolated for the experiments across 10 sessions. As has been done many times previously, isolated units were categorized as being either putative pyramidal neurons or putative interneurons on the basis of wave shape and average inter-spike interval (e.g., Bartho et al., 2004; Sirota et al., 2008).

*Statistical analysis of neural data*

*"Taste responsiveness"*. A single neuron was deemed "taste-responsive" if it showed differential firing rates before and after taste delivery. Paired t-tests were conducted to determine whether the evoked firing rate (2 seconds post-delivery) significantly differed from its baseline firing rate (2 seconds prior taste delivery). Alpha level was set at $p < 0.05$. This analysis was first performed on firing averaged across taste (providing a general quantification of the neuron's sensitivity to taste input) and then again for each

individual taste response. While this results in a relatively large number of statistical comparisons (a common issue for studies of simple coding), the more unified, more conservative analyses described below were ultimately used for determining the nature of mouse GC taste coding.

*"Taste specificity".* Using the above analysis, it is possible to estimate to how many tastes a neuron responds. This fails to provide a rigorous description of the taste-specificity of the neuron's firing, however; concluding differences between responses on the basis of separate tests ("because the neuron responds to both X and Y, its responses to X and Y are the same" or "because the neuron responds significantly to X but not to Y, its responses to X and Y are significantly different") is statistically invalid (Nieuwenhuis, et al., 2011). We therefore tested whether a single-neuron's responses were "taste specific" *via* direct comparison of the firing rates elicited by the 4 tastes. Specifically, post-delivery firing rates were divided into four consecutive 500-ms bins, and a mixed-design ANOVA was conducted with Taste as the between-subject variable and Time as the within-subject variable; a neuron's responses were categorized as taste-specific if either the main effect of Taste or the Taste X Time interaction was significant ($p < 0.01$). The former significant effect connoted simple taste specificity—at least one taste induced an amount of spiking that differed significantly from that driven by at least one other taste—and the latter connoted "temporal coding"—a Taste x Time interaction implies that the time course of the response to one taste was different from the time course of the response to at least one other taste (note that a set of responses could be identical in average rate but differ in time course, whereby the Taste main effect would be non-significant and the Taste x

Time interaction would be significant). Post-hoc tests (Tukey's HSD) revealed precisely which responses differed.

*"Entropy (H)".* We employed the oft-used metric of entropy (H) as a direct evaluation of the breadth of single-neuron tuning. H was computed as previously reported by Smith and Travers (1979) using the following formula:

$$H = -K \sum_{i=1}^{n} Pi \log Pi,$$

where K is a constant, and P is the proportional response to each taste (i). A low H value indicates higher selectivity (H=0 for a unit that only responds to one taste), whereas a high H value represents broader tuning (H=1 for a unit responding to all tastes). Taste evoked responses were calculated by subtracting mean firing rates of pre-taste delivery (2 seconds) from post-taste taste delivery (2 seconds).

Note that these three analyses combine to provide a rich description of GC neuron taste-responsiveness. For instance, a neuron could conceivably respond to all tastes equally; this neuron would have high entropy and broad taste responsiveness, but would likely be responding not to taste quality *per se* but to some other aspect of the stimulus. Accordingly, its firing would almost certainly fail to be deemed taste-specific according to the Taste main effect in a 2-way ANOVA.

Finally, it is worth noting that an H calculated to be somewhere between 0 and 1 can conceivably be described to represent "broad" or "narrow" coding, depending upon one's perspective. To enhance interpretability of H distributions, we therefore compared our results to those of identical analyses performed on simulated datasets (created based on the real data) made up of units with known breadth.

*"*Time course of palatability-related responding." Taking a cue from our work on rats (e.g., Fontanini et al., 2009; Piette et al., 2012; Sadacca et al., 2012; Li et al., 2016; Sadacca et al., 2016), we used a moving-window analysis to identify the times at which GC taste responses reflected the hedonic value of the tastes. We first ranked the taste stimuli based on their palatability (see below); the ranking of palatability of tastes used herein is, from highest to lowest, sucrose, NaCl, citric acid and quinine. We then, for each window of neural firing (window size: 250 ms; step size: 25 ms), we performed a (Pearson product-moment) correlation between the firing rates to each taste and the palatability rankings. Because this procedure results in a relatively large number of actual tests, we limited the chances of Type I errors by concluding that the responses were palatability-related only when the test achieved significance for 3 consecutive bins.

*Taste palatability assessment*

To determine the palatability of each of the taste used in this study, mice (N=32; a separate set from those used in the electrophysiology experiment) were mildly water restricted for 3 days (one 30-min period of access to water in the morning, and in the afternoon). One the next day, mice were exposed to one of the tastes (sucrose, NaCl, citric acid, or quinine) for 30-min, and consumption of the tastes was measured by weighting the bottle before and after the drinking session. While our use of these data does not depend on the significance of consumption decisions (in fact, if no structural differences in consumption existed, it would be vanishingly unlikely that there would be significant correlations between the essentially random ranking and neural coding), a one-way ANOVA revealed strong inter-stimulus differences in consumption ($F(3,28) = 32.97$, $p < 0.01$).

*Modeling and change-point identification in ensemble firing data*

GC taste processing is dynamic—rat responses have been shown to undergo a pair of sudden and coherent firing-rate transitions in the 1.5 sec post-delivery; the state prior to the first transition is the same for all tastes, reflecting taste 'detection;' the states attained following the first and second transitions are both taste-specific, with the last further reflecting taste palatability. In order to detect whether such transitions between states occur in mouse GC, we performed a simple change-point analysis on ensemble spike data. This analysis is summarized here; for complete details, see Mukherjee et al. (2018).

Trials of ensemble spiking data were categorized in terms of which neuron spiked in each 1-ms bin; an index of 0 corresponded to no spikes from any neuron. If more than one neuron spiked in a time bin—a highly uncommon occurrence, given the relatively low firing rates of GC neurons—we randomly selected one spiking neuron to index that bin (Jones et al., 2007; Sadacca et al., 2016). We then fit a change-point model describing ensemble firing rate transitions between the 3 states as categorical distributions with emissions. We constrained the model on the basis of the findings described above, and performed tests to ensure that this constrained model accurately reflected the specific dynamics of the real data, specifically asking whether state 3 contained the majority of the palatability-related firing, as predicted on the basis of the rat data.

We analyzed 1.7s of ensemble activity post taste delivery, constraining the change from state 1 to state 2 (change-point 1, or CP1) to happen within the interval [50 – 600 ms]. The second change-point (CP2) was constrained to occur within the interval [CP1 + 0.2s to 1500ms. This is equivalent to placing uniform priors over the intervals that define

CP1 and CP2, corresponding to the timing of sudden, coherent firing rate transitions in GC ensembles (Jones et al., 2007, Sadacca et al., 2016). With these assumptions, the Expectation-Maximization (EM) algorithm, the most widely used approach to perform inference in such models with latent variables (CP1 and CP2), was employed to fit the change-point model (Bishop, 2016).

*Histology*

At the end of each experiment, mice were deeply anesthetized and perfused transcardially with 0.9 % saline for 1 minute followed by 4% paraformaldehyde. Brains were extracted and post fixed in 4% paraformaldehyde for 24-48 hours, after which coronal brain slices (60 µm) containing the GC were sectioned on a vibratome. Sections were rinsed 5-6 times over 90 mins (PBS/.3% Triton X-100), mounted on charged glass slides, and cover slipped with mounting medium including DAPI (Vectashield). The placement of electrodes was determined by localizing Dil (a lipophilic dye coated on electrodes during implantation). To visualize electrode bundle locations, bilateral GC sections were viewed by confocal fluorescence microscopy with a Leica Sp5 Spectral confocal microscope/Resonant Scanner with 405 (for DAPI), 546 (Dil dye) and 488 (for GFP) lasers equipped with x/y/z movement stage.

## Results

We recorded the spiking of ensembles of single murine gustatory cortical (GC) neurons, using bilaterally implanted electrode bundles, in response to a stimulus battery representing four major taste modalities (sweet: 0.2 M sucrose, salty: 0.1 M sodium-chloride, sour: 0.02 M citric-acid and bitter: 0.001 M quinine; see Figure 5 for behavioral characterization, which is essentially identical to the preferences of rats) delivered *via* intra oral cannula (15 deliveries of 15 µl).

A total of 185 units were isolated across 10 sessions in 6 mice—4 mice received 2 sessions each (in the latter case sessions were recorded from separate DV locations in the GC; see material and methods). As shown in Figure 1, our recordings spanned much of the region (AP Bregma +1.6 to 0.0; DV 2.25 – 3.25 mm from the surface of the brain) receiving input from taste thalamus (Chen et al., 2011; Fletcher et al., 2017) or from the amygdala (Matyas etal., 2014); prior work has shown this region to be important for taste behavior and learning in mice (Neseliler et al., 2011).

### Basic characterization of taste evoked responses in the gustatory cortex of mice

Figure 2 presents raster plots and associated PTSHs for the taste responses of three simultaneously recorded GC neurons. The first two are regularly spiking (putative) pyramidal neurons and the third is a fast-spiking (putative) inhibitory interneuron. Each neuron's responses were significantly (see Methods) taste-specific: Unit 1 responded to all 4 tastes, but responded more strongly to NaCl and sucrose than to the remaining tastes; Unit 2, on the other hand, responded strongly to sucrose, citric acid, and quinine,

but far less to NaCl; Unit 3, meanwhile, was inhibited to differing degrees and for differing lengths of time by all 4 tastes.

Even the most basic analysis of these responses (i.e., analyzing average firing rates, and ignoring differences in temporal coding) revealed, consistent with what has been reported in awake rats (Piette et al., 2012; Moran and Katz, 2014), that a large percentage (just under 2/3) of mouse GC neurons respond to taste stimulation (significant paired t-tests comparing pre- to post-stimulus firing across all trials summed across tastes, Figure 3A). Excitatory responses (enhanced firing) outnumbered inhibitory (reduced firing) almost 3 to 1. Examination of the taste-specificity of that firing (using ANOVAs to directly compare a neuron's response to different tastes, and including time as a 2$^{nd}$ factor), identified an almost identical percentage of neurons as being "taste neurons" (i.e., responding distinctly to at least one taste, see Methods and Figure 3C). While these two analyses may not necessarily identify precisely the same neurons (see Methods), together they suggest that the vast majority of "taste responses" in mouse GC are truly taste-related, as opposed to reflecting somatosensory or general cognitive factors.

While taste-specific, these responses were broad (i.e., significant firing rate modulations in individual neurons were seldom restricted to only one, or even two, of the four basic tastes delivered). Had they been narrow, then the rate of significant responses to each individual taste (determined using simple t-tests, as above, applied to each individual PSTH) would be expected to be around ¼ of this 66% (that is, we'd expect ~16% of the neurons to have sucrose responses, another ~16% to have NaCl responses, etc). Our analysis, however, revealed a far higher percentage of neurons as responding to each

taste (Figure 3B), a result that suggested that most taste neurons in mouse GC must respond to > 1 taste on average.

We performed multiple convergent tests of this conclusion. First, we directly analyzed the number of tastes that evoked significant responses in each recorded neuron (pre- vs post-stimulus t-tests). This analysis revealed that 28.6% of our mouse GC neurons responded significantly to one taste; 25.6% responded to two tastes, 16.8% to three tastes, and 14.1% to all four tastes (Figure 4A). While it is inappropriate to reach conclusions concerning taste specificity from this method (which does not directly compare responses to different tastes, see Methods), these results confirm that the majority of GC neurons that respond to taste stimulation respond to > 1 taste.

We went on to calculate response entropy (H) for each neuron, using standard techniques (Smith and Travers., 1979; Samuelsen et al., 2013); low H values indicate narrowly responsive neurons, and high H values indicate broadly tuned neurons. The distribution for our neural sample proved to be highly positively skewed, with the vast majority of GC neurons' H values suggesting broad responsiveness; the distribution was similar when only neurons identified as responding in a taste-specific manner were included (Figure 4B).

To enhance the interpretability of this result (see Methods), we have also plotted the H values of a simulated set of neurons that all responded to only one taste: this distribution is significantly different from the distribution of the real data ($X^2 = 82.75$, $p < 0.01$) which most resembles (according to Kullback-Leibler divergence) data from neural data simulated to have responses to 3 to 4 tastes (Figure 4C).

**Dynamics of taste-evoked responses in mice GC**

The above data suggest that GC taste neurons are broadly tuned "coarse coders," responding distinctly to multiple tastes; as such, they are consistent with previous reports of taste responses in rat GC (Yamamoto et al., 1985; Bahar et al., 2004; Fontanini and Katz., 2006; Jones et al., 2007; Piette et al., 2012; Samuelsen et al., 2013), and with calcium imaging data from mouse GC (Fletcher et al., 2017; but see Chen et al., 2011). But the prior work on rats further demonstrates that such analyses are inadequate to describe GC taste responses, in that they ignore meaningful response changes that occur across the first 1.5s of post-stimulus time (the period leading up to the making of consumption decisions and production of consumption-related behaviors, see Grill & Noregren, 1978; Travers and Norgren., 1986; Li et al., 2016). The complete range of the information carried in rat GC taste responses can be appreciated only when reliable, phasic modulations of firing rate—the temporal dimension of taste responses—are considered (Katz et al., 2001; Fontanini & Katz, 2006; Piette et al., 2012; Sadacca et al., 2012; Maier & Katz, 2013; Li et al., 2016; Baez-Santiago et al., 2016).

Fine-grained analysis of mouse GC taste PSTHs suggests the presence of interpretable firing-rate dynamics, with response magnitudes changing through time in taste-specific manners. An example is shown in Figure 5A—a mouse GC neuron that responded strongly to NaCl during the 1$^{st}$ post-delivery second only, and strongly to citric acid during the 2$^{nd}$ post-delivery second only (note that when this pattern of firing is averaged across time, the neuron incorrectly registers as responsive to quinine only, once again

demonstrating the inadequacy of that earlier analysis for the purposes of characterizing the taste-specificity of firing).

To evaluate the temporal evolution of these responses in relation to the sensory and psychological properties of taste perception, we first ascertained mouse behavioral preferences for our battery of four tastes (which differed in both chemical identity and palatability, sucrose and sodium-chloride representing palatable tastes and citric acid and quinine representing non-palatable tastes) using a single-bottle consumption test. We then correlated this vector of palatabilities with the vector of firing rates to the same battery of tastes in small bins of the 2-sec response epoch (using a moving-window analysis as explained in the Methods and used previously in Fontanini et al., 2009; Piette et al., 2012; Sadacca et al., 2012; Li et al., 2016; Sadacca et al., 2016). An example of the result of this analysis is shown in Figure 5A2 (with the taste preference data presented as an inset): for this single neuron, firing did not become significantly palatability-related (green dots) until several hundred msec after the onset of taste responsiveness, and reached a peak of palatability-relatedness a full sec after taste delivery; inspection of Figure 5A1 suggests that the responses were taste-specific prior to the emergence of palatability-relatedness, but that firing rates shifted between 0.5 and 1.0 sec into the response such that the order of response magnitudes came to reflect palatability (in this case the ordering was “aversive high,” which appeared with approximately the same frequency in our neural sample as “aversive low”).

Figure 5B, which presents the results of this analysis performed upon the entire data set, confirms the representativeness of the example: the incidence of taste specificity rises almost immediately following taste stimulus delivery, and approaches peak levels as early

as 500 ms into the response; palatability relatedness, on the other hand, rises more slowly, beginning to trend upward ~500 ms after stimulus delivery and approaching a peak at ~1000 ms into the response.

We performed one further test of this result, analyzing the distinctiveness of different subsets of taste responses for each neuron at each point in response time. “Distinctiveness” was quantified in terms of normalized Euclidean distances separating two taste responses in a multi-dimensional scaling solution. Given the above results, we predicted that the distinctiveness of individual pairs of tastes would rise quickly, but that the difference between palatabilities—that is, comparing the averaged responses to the palatable tastes (sucrose and NaCl) to the averaged responses to the aversive tastes (quinine and citric acid)—would emerge only later. Figure 5C reveals that this is precisely what we observed: the separation of codes for sucrose and NaCl (yellow line ± SE) rose quickly in post-delivery time, as did the separation of codes for quinine and citric acid (beige line ± SE); the rise in the separation between palatabilities (green line ± SE), meanwhile, was delayed. Following the rise of palatability discriminability, the discriminability of individual “same-palatability” taste pairs fell precipitously, confirming that general taste-specificity becomes refined across time into palatability-relatedness.

Thus, we conclude that mouse GC codes taste properties sequentially across 1.5 seconds of post-stimulus time, with taste-specificity appearing prior to palatability-relatedness. Ancillary analysis confirms that many individual neurons respond distinctly in the two epochs, coding both taste identity early and taste palatability late. In fact, 50% of the neurons that produce significantly taste-specific firing also produce significantly palatability-related firing (as in the example neuron shown in Figure 5a).

**Ensemble properties of murine cortical taste dynamics**

Having established the existence of reliable, interpretable single-neuron dynamics in mouse GC, we moved on to asking whether in mice, as is true in rats, these single-neuron dynamics are in fact reflections of coherent ensemble activity. As we have done with rat data (Mukherjee et al., under review), we applied change-point modeling (see Methods) procedures to datasets comprised of simultaneously-recorded neural ensembles, to test whether firing rate transitions between epochs are: 1) coherent between neurons; 2) sudden; and 3) trial-specific in latency.

Our analysis, which is summarized in Figure 6, suggests that they are, and in the process demonstrates further features of the taste code in mouse GC. Figure 6A shows an example of 3 sucrose trials; a one-way ANOVA revealed that the palatability correlation varied with Epoch ($F$ = 24.36, $p$ < 0.01), and post-hoc comparisons revealed that this significance is largely driven by the fact that the correlation with palatability is significantly higher following the second transition than before ($p$ < .05). The fact that palatability correlations are modestly higher following the first transition than before reflects the simple fact that the very earliest 100-200ms of GC responses (i.e., those preceding even the 1$^{st}$ transition) are, as they are in rats, totally non-specific; almost any taste specificity will enhance correlations with palatability beyond those chance correlations observed with non-specific firing.

The average transition times for CP1 and CP2 occurred at ~190 ms and ~800 ms, respectively (Figure 6C). Note that these average transition times were not centered on

the middle of the available intervals (which were 325 and 925ms, respectively; see Methods), a fact that is inconsistent with the hypothesis that they are simply artifacts of the procedure itself; rather, these latencies are good matches for our prior rat data, and for our single-neuron results (Fig 5D), and confirm our expectation that mouse GC ensembles undergo fairly sudden and coherent shifts in firing while responding to tastes.

These results further suggest that single-neuron dynamics in mouse GC, as described above, fail to completely characterize taste processing (as is also true in rats). Rather than acting as independent elements, they are likely reflections of population coding—an unsurprising fact given the mesoscopic (intracortical connectivity) and macro-scopic (between-region feedback) circuitry involved in taste.

**Spatial analysis of murine cortical taste response properties**

GC is a distributed, inhomogeneous region that can be subdivided according to cytoarchitectural and connectivity criteria in the dorsal-ventral (into granular, dysgranular and agranular regions) and anterior-posterior axes (Allen et al., 1991; Maffei et al., 2012). One subset of the imaging literature has suggested that mouse cortical taste coding, unlike that of rat (Accolla et al., 2007), is cleanly gustotopic (Chen et al., 2011; Wang et al., 2018), while a separate subset suggests otherwise (Fletcher et al., 2017).

To explore the potential spatial dependencies of GC taste coding using electrophysiology (which is far more sensitive to subtle firing rate changes), we compared taste-evoked responses along the two primary axes of GC. In the dorsal-ventral dimension we were able to look within-subject, as our electrode bundles could be driven ventrally between

tasting sessions. Figure 7 shows a pair of example neurons recorded from dorsal GC, and a second pair recorded from ventral GC in the same mouse. It can be seen that each of these responses are quite broad, suggesting basic similarities between dorsal and ventral GC.

Closer analysis confirmed the similarity of different recording depths. Analysis of the entire sample divided into dorsal and ventral recordings revealed no striking differences in breadth of responsiveness, measured either in terms of number of tastes responded to (Figure 8a, $X^2 = 1.15$, $p = 0.885$) or response entropy (Figure 8b; $X^2 < 1$). The magnitudes of taste specificity revealed by ANOVA was similar across dorsal and ventral neurons (Fig. 8C; $F < 1$), and the pattern of how many neurons responded to which taste did not differ significantly between subregion (Figure 8D); in both dorsal and ventral GC, single neurons were more likely to respond to both palatable and aversive neurons than either alone (data not shown). Finally, dorsal and ventral neural samples showed similar time-courses of response evolution from quality to palatability, measured in terms of the number of neurons showing such responses at each time point (Figure 8D1-2).

In the anterior-posterior dimension, our results were analogous. We compared taste responses between bregma +1.6 and bregma 0.0, treating everything forward of 0.8 as “anterior.” This analysis also revealed no aspects of taste coding that varied notably with anatomical location: we saw no significant differences between anterior/posterior breadth of responsiveness, measured either in terms of number of tastes responded to (Figure 9A, $X^2 = 5.51$, $p = 0.239$) or response entropy (Figure 9B; $X^2 < 1$); furthermore, neurons from anterior and posterior GC subdivisions had similar magnitudes of taste specificity (Figure 9C; $F < 1$), similar patterns of how many neurons responded to each taste (Figure

9D), and similar time-courses of response evolution from quality to palatability (Figure 9D1-2).

Together these results suggest that taste coding is relatively invariant to anatomical location within mouse GC – neurons across the anterior-posterior and dorsal-ventral axes code all taste modalities in a broad and temporally complex manner. Of course, the lack of significant difference does not equal rigorously identified “sameness,” and the possibility remains that subtle differences between anatomical subregions (or between species, for that matter) remain to be identified. Nonetheless, these analyses fail to reveal major differences in taste coding across the breadth of mouse GC.

## Discussion

Mice have become the most common non-human mammalian species studied by neuroscientists—a fact that can no doubt be attributed to the accessibility of mouse genetics, which allows researchers to (relatively) easily study the underlying molecular mechanisms of cellular, network, and behavioral phenomena (Stevens, 1996; Kandel et al., 2014). As the sense with (arguably) the tightest link to behavior and learning (Carleton et al., 2010; Maffei et al., 2012; Katz & Sadacca, 2010), taste is a particularly good system with which to study these topics in a unified manner. Furthermore, this work can take advantage of the extensive progress that has been made toward understanding key principles of taste coding in awake rats (Accolla et al., 2007; Bahar et al., 2004; Fontanini and Katz., 2006; Jones et al., 2007; Katz et al., 2001; Li et al., 2016; Moran & Katz., 2014; Sadacca et al., 2012; Samuelsen et al., 2012). It is somewhat surprising, therefore, that there has been almost no electrophysiological work done on mouse cortical taste coding, and that the imaging studies performed thus far have failed to provide consensus on basic features of gustatory sensory coding (Chen et al., 2011; Fletcher et al., 2017).

In fact, the current study represents one of the first thorough investigations of single-neuron spiking responses in mouse primary gustatory cortex (GC, but see Kusamoto-Yoshida et al, 2015). Using a battery of four basic tastes (sweet, salty, sour and bitter) delivered directly to the tongue of freely moving mice, in conjunction with a multi-electrode bundle designed to record the activity of small ensembles of single neurons, we show that mouse GC codes taste in a largely non-sparse manner: approximately 2/3 of recorded GC responses conveyed information about taste identity, and by and large, these responses were broadly tuned—over half of the recorded neurons responded to >

1 taste, and over half of taste neurons produced firing patterns that were distinctive for 3 of 4 tastes.

But the taste responses of murine GC neurons, while broad, are not unstructured; rather, they evolve in a characterizable way across 1-1.5 seconds. By using a battery of tastes with a range of both chemical identities and palatabilities, we were able to identify separate “epochs” of GC responses related to each property. A large portion (50%) of the recorded neurons coded stimulus identity and stimulus palatability sequentially, rather than being active in only one coding epoch; in fact, transitions between response epochs could be observed in single trials using ensemble statistics. These results suggest that the processing of quality and palatability is likely not performed by independent neural ensembles.

In all of these results, we observed a striking similarity between mouse cortical taste coding and that extensively described in rat data (Accolla et al., 2007; Bahar et al., 2004; Fontanini and Katz., 2006; Jones et al., 2007; Piette et al., 2012; Sadacca et al., 2012; Samuelsen et al., 2013; Yamamoto et al., 1985). Both species code tastes broadly, and these codes reflect identity and taste palatability in separate, sequential epochs. We found no striking qualitative differences between mouse and rat in basic coding, a fact that is unsurprising given that the anatomy of the two species’ taste systems, from the molecular to the macroscopic and from the periphery to the cortex, appears similar. It may well be that differences will emerge with regard to the impact of taste learning on neural coding (which we will examine in the future); there are several notable differences in the way that rats and mice appear to learn conditioned taste aversions, for instance, that could well be reflected in electrophysiological responses.

It was important that we extend our analyses into the spatial domain (a possibility that was not addressed in our work on rat GC), probing for possible differences in how dorsal/ventral and anterior/posterior subregions of GC code tastes, because: 1) GC subregions form distinct connections with other brain regions along the dorsal/ventral and anterior/posterior axes (Allen et al., 1991; Haley, et al., 2016; Maffei et al., 2012); and 2) discrepancies within the literature on imaging of mouse GC (Chen et al., 2011; Livneh et al., 2016; Fletcher et al., 2017). Our comparisons revealed remarkable spatial invariance of coding, consistent with Fletcher et al (2017; see also Accolla et al., 2007)—neurons across the heart of GC produced similarly broad, temporally complex taste responses.

This invariance in the face of non-uniform input—most notably, dorsal GC receives mainly thalamic input whereas ventral GC receives mainly amygdala input, the latter of which is important for palatability coding (Piette et al., 2012)—suggests that GC taste responses are to a large extent a function of distributed cortical network processing, rather than of direct sensory or effective input. This interpretation is supported by the finding that GC neurons code multiple aspects of tastes in a temporally distributed fashion, which suggests convergence of pathways, and population coding analysis that reveal the temporal codes to be a reliable sequence of coherent network states (see Grossman et al., 2008; Jones et al., 2007; Moran & Katz, 2014; Sadacca et al., 2016). Together our results provide insight about the structure of taste coding in mice, and provide an entrée into the unified study of relationship between molecular and network underpinnings of perception and behavior.

References


Allen GV, Saper CB, Hurley KM, Cechetto DF (1991) Organization of visceral and limbic connections in the insular cortex of the rat. J Comp Neurol 311:1-16.

Accolla R, Bathellier B, Petersen CC, Carleton A (2007) Differential spatial representation of taste modalities in the rat gustatory cortex. J Neurosci 27:1396-1404.

Bahar A, Dudai Y, Ahissar E (2004) Neural signature of taste familiarity in the gustatory cortex of the freely behaving rat. J Neurophysiol 92:3298-3308.

Baez-Santiago MA, Reid EE, Moran A, Maier JX, Marrero-Garcia Y, Katz DB (2016) Dynamic taste responses of parabrachial pontine neurons in awake rats. J Neurophysiol 115:1314-1323.

Bartho P, Hirase H, Monconduit L, Zugaro M, Harris KD, Buzsaki G (2004) Characterization of neocortical principal cells and interneurons by network interactions and extracellular features. J Neurophysiol 92:600-608.

Carleton A, Accolla R, Simon SA (2010) Coding in the mammalian gustatory system. Trends Neurosci 33:326-334.

Chen X, Gabitto M, Peng Y, Ryba NJ, Zuker CS (2011) A gustotopic map of taste qualities in the mammalian brain. Science 333:1262-1266.

Fletcher ML, Ogg MC, Lu L, Ogg RJ, Boughter JD, Jr. (2017) Overlapping Representation of Primary Tastes in a Defined Region of the Gustatory Cortex. J Neurosci 37:7595-7605.

Fontanini A, Grossman SE, Figueroa JA, Katz DB (2009) Distinct subtypes of basolateral amygdala taste neurons reflect palatability and reward. J Neurosci 29:2486-2495.

Fontanini A, Katz DB (2006) State-dependent modulation of time-varying gustatory responses. J Neurophysiol 96:3183-3193.

Grossman SE, Fontanini A, Wieskopf JS, Katz DB (2008) Learning-related plasticity of temporal coding in simultaneously recorded amygdala-cortical ensembles. J Neurosci 28:2864-2873.

Haley MS, Fontanini A, Maffei A (2016) Laminar- and Target-Specific Amygdalar Inputs in Rat Primary Gustatory Cortex. J Neurosci 36:2623-2637.

Haslinger R, Ulbert I, Moore CI, Brown EN, Devor A (2006) Analysis of LFP phase predicts sensory response of barrel cortex. J Neurophysiol 96:1658-1663.

Jezzini A, Mazzucato L, La Camera G, Fontanini A (2013) Processing of hedonic and chemosensory features of taste in medial prefrontal and insular networks. J Neurosci 33:18966-18978.

Ji D, Wilson MA (2007) Coordinated memory replay in the visual cortex and hippocampus during sleep. Nat Neurosci 10:100-107.

Jones LM, Fontanini A, Sadacca BF, Miller P, Katz DB (2007) Natural stimuli evoke dynamic sequences of states in sensory cortical ensembles. Proc Natl Acad Sci U S A 104:18772-18777.

Kandel ER, Dudai Y, Mayford MR (2014) The molecular and systems biology of memory. Cell 157:163-186.

Katz DB, Simon SA, Nicolelis MA (2001) Dynamic and multimodal responses of gustatory cortical neurons in awake rats. J Neurosci 21:4478-4489.

Kimura Y, Jacobs LL, Cerling TE, Uno KT, Ferguson KM, Flynn LJ, Patnaik R (2013) Fossil mice and rats show isotopic evidence of niche partitioning and change in

dental ecomorphology related to dietary shift in Late Miocene of Pakistan. PLoS One 8:e69308.
Kusumoto-Yoshida I, Liu H, Chen BT, Fontanini A, Bonci A (2015) Central role for the insular cortex in mediating conditioned responses to anticipatory cues. Proc Natl Acad Sci U S A 112:1190-1195.
Lavi K, Jacobson GA, Rosenblum K, Luthi A (2018) Encoding of Conditioned Taste Aversion in Cortico-Amygdala Circuits. Cell Rep 24:278-283.
Li JX, Yoshida T, Monk KJ, Katz DB (2013) Lateral hypothalamus contains two types of palatability-related taste responses with distinct dynamics. J Neurosci 33:9462-9473.
Li JX, Maier JX, Reid EE, Katz DB (2016) Sensory Cortical Activity Is Related to the Selection of a Rhythmic Motor Action Pattern. J Neurosci 36:5596-5607.
Maffei A, Haley M, Fontanini A (2012) Neural processing of gustatory information in insular circuits. Curr Opin Neurobiol 22:709-716.
Maier JX, Katz DB (2013) Neural dynamics in response to binary taste mixtures. J Neurophysiol 109:2108-2117.
Matyas F, Lee J, Shin HS, Acsady L (2014) The fear circuit of the mouse forebrain: connections between the mediodorsal thalamus, frontal cortices and basolateral amygdala. Eur J Neurosci 39:1810-1823.
Moran A, Katz DB (2014) Sensory cortical population dynamics uniquely track behavior across learning and extinction. J Neurosci 34:1248-1257.
Mukherjee N, Wachutka J, Katz DB (2017) Python meets systems neuroscience: affordable, scalable and open-source electrophysiology in awake, behaving rodents. In Proceedings of the 16th Python in Science Conference, 98 – 105.
Mukherjee N, Wachutka J, Katz DB. (2018) Dynamical structure of cortical taste responses revealed by precisely-timed optogenetic perturbation. bioRxiv.
Neseliler S, Narayanan D, Fortis-Santiago Y, Katz DB, Birren SJ (2011) Genetically induced cholinergic hyper-innervation enhances taste learning. Front Syst Neurosci 5:97.
Nieuwenhuis S, Forstmann BU, Wagenmakers EJ (2011) Erroneous analyses of interactions in neuroscience: a problem of significance. Nat Neurosci 14:1105-1107.
Peng Y, Gillis-Smith S, Jin H, Trankner D, Ryba NJ, Zuker CS (2015) Sweet and bitter taste in the brain of awake behaving animals. Nature 527:512-515.
Piette CE, Baez-Santiago MA, Reid EE, Katz DB, Moran A (2012) Inactivation of basolateral amygdala specifically eliminates palatability-related information in cortical sensory responses. J Neurosci 32:9981-9991.
Sadacca BF, Rothwax JT, Katz DB (2012) Sodium concentration coding gives way to evaluative coding in cortex and amygdala. J Neurosci 32:9999-10011.
Sadacca BF, Mukherjee N, Vladusich T, Li JX, Katz DB, Miller P (2016) The Behavioral Relevance of Cortical Neural Ensemble Responses Emerges Suddenly. J Neurosci 36:655-669.
Samuelsen CL, Fontanini A (2017) Processing of Intraoral Olfactory and Gustatory Signals in the Gustatory Cortex of Awake Rats. J Neurosci 37:244-257.
Samuelsen CL, Gardner MP, Fontanini A (2012) Effects of cue-triggered expectation on cortical processing of taste. Neuron 74:410-422.

Samuelsen CL, Gardner MP, Fontanini A (2013) Thalamic contribution to cortical processing of taste and expectation. J Neurosci 33:1815-1827.

Smith DV, Travers JB (1979) A metric for the breadth of tuning of gustatory neurons. Chem Senses 4:215–229.

Sirota A, Montgomery S, Fujisawa S, Isomura Y, Zugaro M, Buzsaki G (2008) Entrainment of neocortical neurons and gamma oscillations by the hippocampal theta rhythm. Neuron 60:683-697.

Stevens CF (1996) Spatial learning and memory: the beginning of a dream. Cell 87:1147-1148.

Talbot ZN, Sparks FT, Dvorak D, Curran BM, Alarcon JM, Fenton AA (2018) Normal CA1 Place Fields but Discoordinated Network Discharge in a Fmr1-Null Mouse Model of Fragile X Syndrome. Neuron 97:684-697 e684.

Trouche S, Perestenko PV, van de Ven GM, Bratley CT, McNamara CG, Campo-Urriza N, Black SL, Reijmers LG, Dupret D (2016) Recoding a cocaine-place memory engram to a neutral engram in the hippocampus. Nat Neurosci 19:564-567.

Whishaw IQ, Metz GA, Kolb B, Pellis SM (2001) Accelerated nervous system development contributes to behavioral efficiency in the laboratory mouse: a behavioral review and theoretical proposal. Dev Psychobiol 39:151-170.

Yamamoto T, Yuyama N, Kato T, Kawamura Y (1985) Gustatory responses of cortical neurons in rats. II. Information processing of taste quality. J Neurophysiol 53:1356-1369.

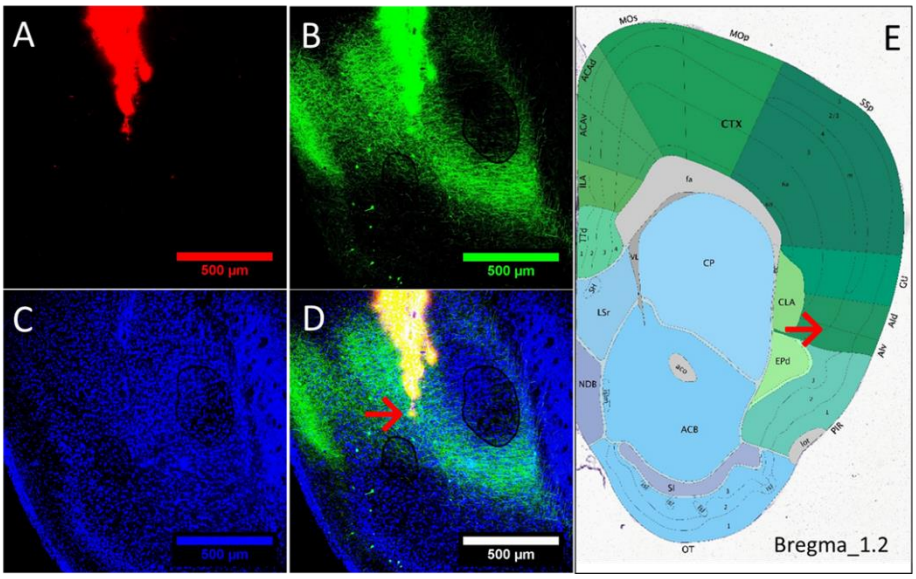


**Figure 1. Localization of electrode bundles in mouse GC**. **A**. To determine the recording site in GC, electrode bundles were coated with Di-I (a red fluorescent tracer) which later showed the track traveled by the multielectrode array in GC (in a mouse that received two recording sessions, see Methods). **B**. Background staining of the same slice with DAPI (a nonspecific nuclear dye). **C**. To assist the separation between dorsal and ventral subregions of GC, BLA was infected with AAV2/5::GFP; resultant GFP-labeled axons were then visible in ventral GC. **D**. In a triple-labeled slice, an arrow indicates the final location of the tips of the electrodes. **E**. A schematic of this slice location (Franklin & Paxinos, 1996) shows the final location of the electrode to be in ventral GC.

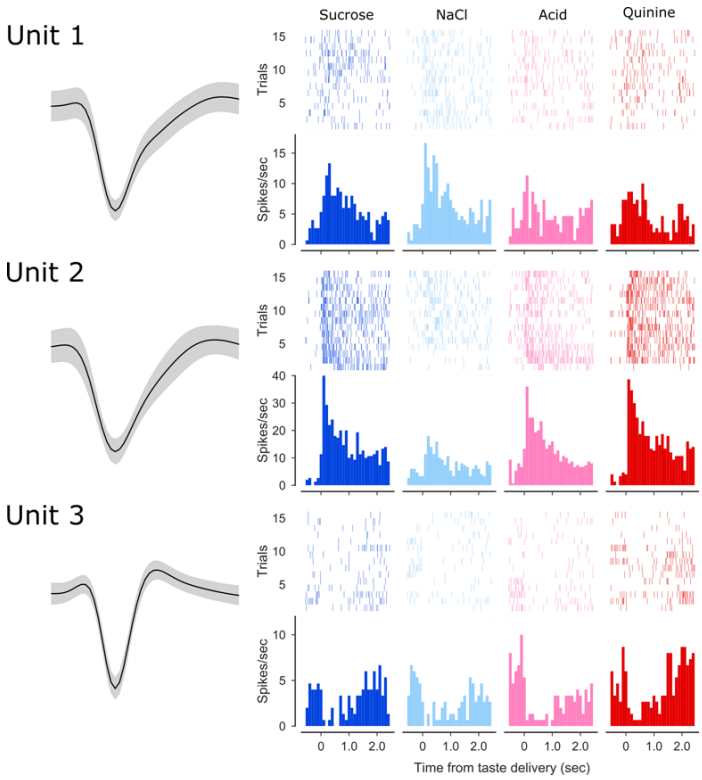


**Figure 2. Simultaneously recorded gustatory cortex neurons**. The left column shows average action potential waveforms (surrounded by confidence intervals) for three neurons recorded simultaneously from the same electrode bundle. The remaining four columns show the responses of these neurons to sweet (sucrose), salty (sodium chloride), sour (citric acid) and bitter (quinine) tastes. The top half of each response display is spike time raster plots (each row is a single trial, and each dot is an action potential), below which are associated PTSHs (firing rate in spike/second in the y-axes; time post-stimulus in the x-axes). Each neuron's responses were taste-specific (see Methods), and each individual neuron responded distinctly.

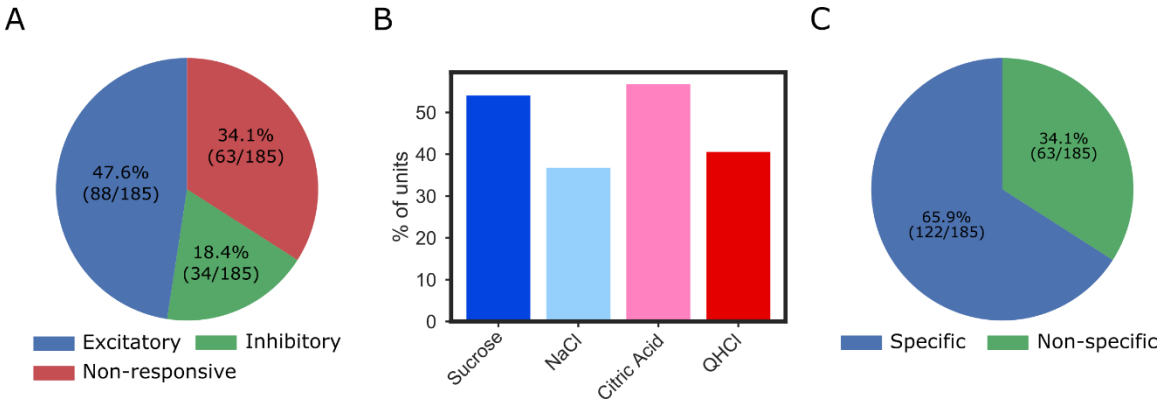


**Figure 3**. **Mouse GC neurons respond to tastes**. **A.** A pie chart showing the percentage and distribution of GC neurons that produced excitatory or inhibitory responses to taste stimulation. **B**. Similar percentages of mouse GC neurons respond to sweet, salty, sour, and bitter tastes; at least 35% of the sample responded to each taste. **C**. 2-way within-neuron ANOVAs comparing responses to the different tastes as a function of time (taste x time, $p<0.01$) revealed that the majority of mouse GC neuron taste responses were also taste-specific (i.e., different for different tastes).

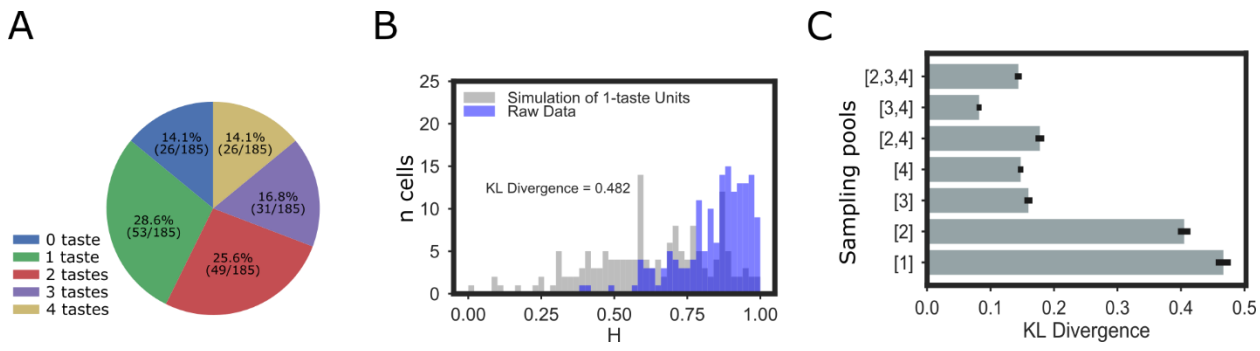


**Figure 4**. **GC neurons code tastes broadly**. **A.** Independent paired t-tests comparing pre- and post-taste firing rates reveal that the majority of mouse GC neurons respond more than one taste (even when totally non-responsive neurons are included in the comparison). **B.** The distribution of the breadth of taste coding (i.e., entropy [H], x-axis) in GC neurons (purple bars, y-axis = 159 of neurons) is highly skewed toward broad tuning (a low H indicates narrowly responsive neuron and a high H indicates a neuron responsive to several tastes). Overlain (grey bars) is the distribution of response entropies for an equivalently-sized set of simulated units which respond to only one taste. The difference of the two distributions was calculated using Kullback-Leibler (KL) divergence, and was highly significant according to a $X^2$ test conducted on the data. **C**. The KL divergences between the collected data and a range of simulated datasets in which units responded to particular numbers of tastes.

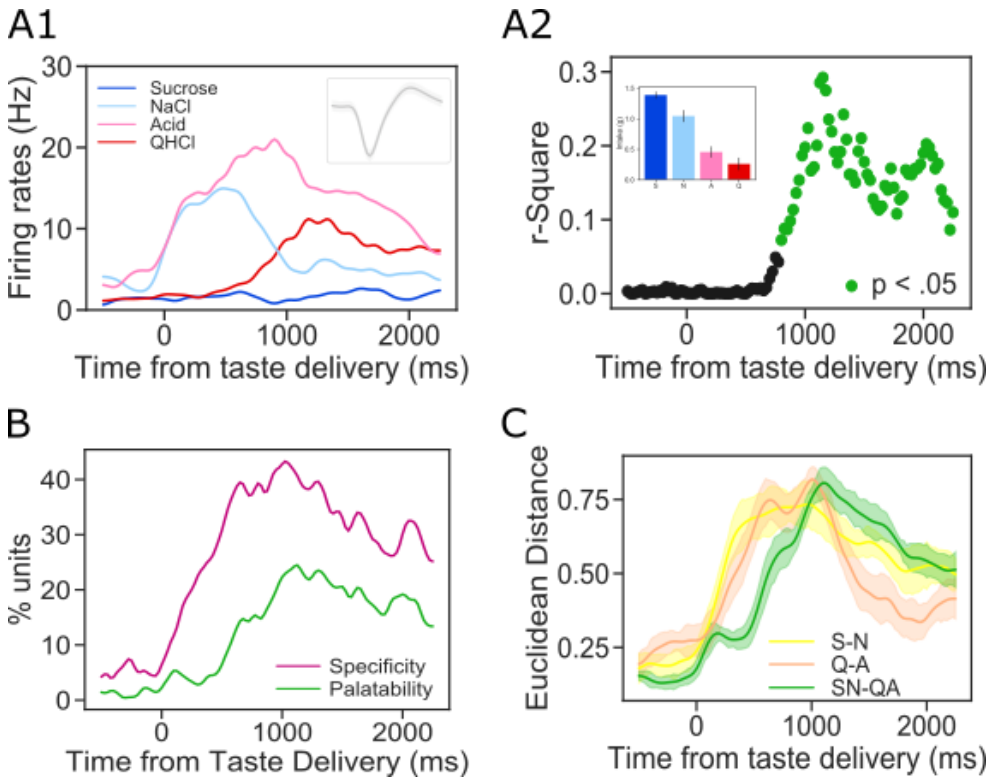


**Figure 5. Murine GC responses evolve through successive epochs of taste quality and taste palatability coding**. **A1**: Overlain PSTHs (y-axis, firing rate; x-axis, time post-stimulus) from a representative GC neuron that responded significantly to all tastes but sucrose [S]. **A2**: Moving window analysis of the correlation (R-squared, y-axis) between firing rates and taste palatability (determined by taste intake, see inset) for the neuron shown in Panel A1. Green dots denote significantly non-zero correlations. **B**. Percentages of the entire sample of GC responses that show significant taste specificity (magenta) and palatability-relatedness (green). Taste specificity starts to rise soon after taste delivery, and peaks at 500ms; in contrast, palatability-related firing appears only following a delay (~500ms), and peaks at ~1 second post-stimulation. **C**. Response differences (euclidean separation in multi-dimensional scaling solutions, see methods for details) between same-palatability tastes qualities (S-N and Q-A) emerge soon after stimulus delivery; between-palatability differences, on the other hand (SN-QA) emerge later, confirming that identity-related activity is followed by palatability-related firing.

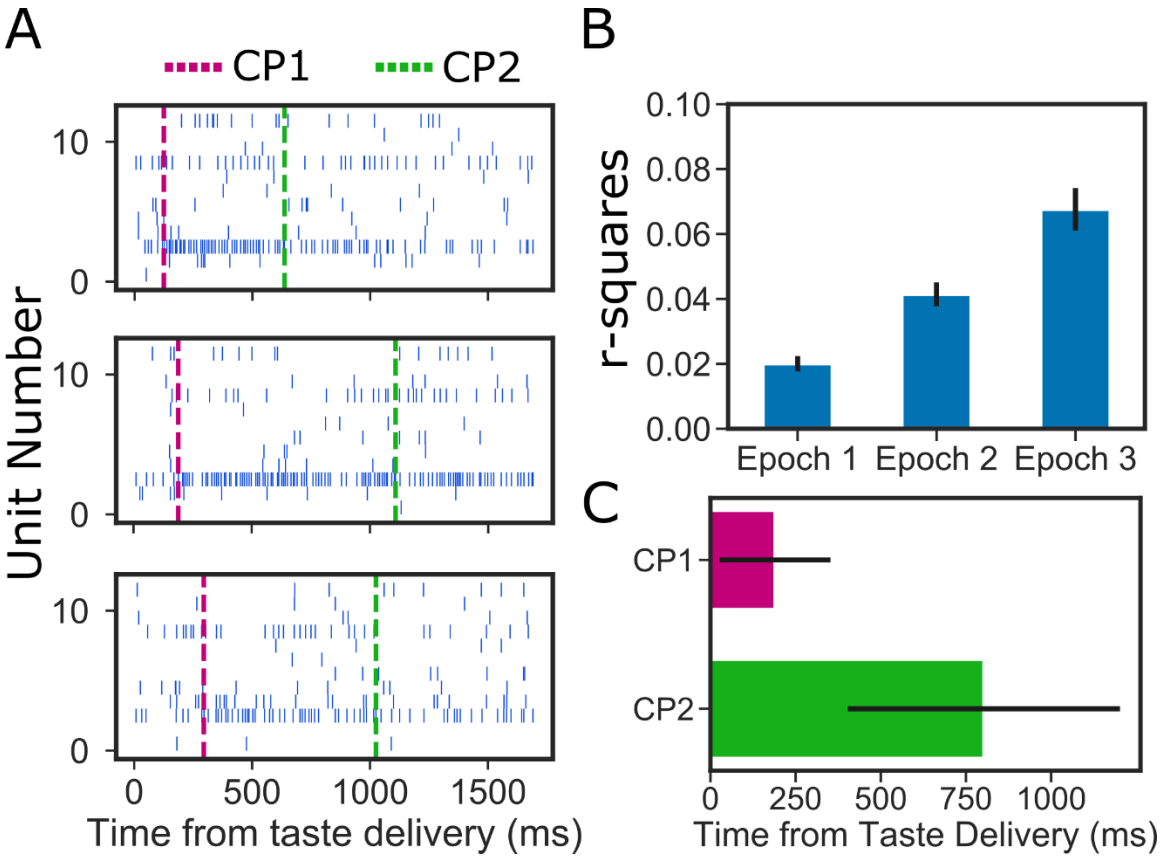


**Figure 6. The epochs of mouse cortical taste responses reflect coherent state sequences in GC ensembles**. **A.** Representative single trials of the response of one GC ensemble (one neuron/row; hash marks = individual action potentials) to the taste of sucrose, revealing sudden, simultaneous changes in firing rates in several neurons. Magenta and green dashed lines indicate the first switch point (CP1: from taste detection to identity) and second switch point (CP2: from taste identity to palatability), respectively. **B.** Correlations between mean firing rates and palatability for each of the three states, demonstrate, consistent with our hypotheses and work on rat GC, that palatability coding is achieved with state 3, and that taste-specificity (which necessarily connotes a basic level of non-zero palatability coding) is achieved with state 2. **C**. Average state-to-state transition times across all trials revealed through switch point analysis.

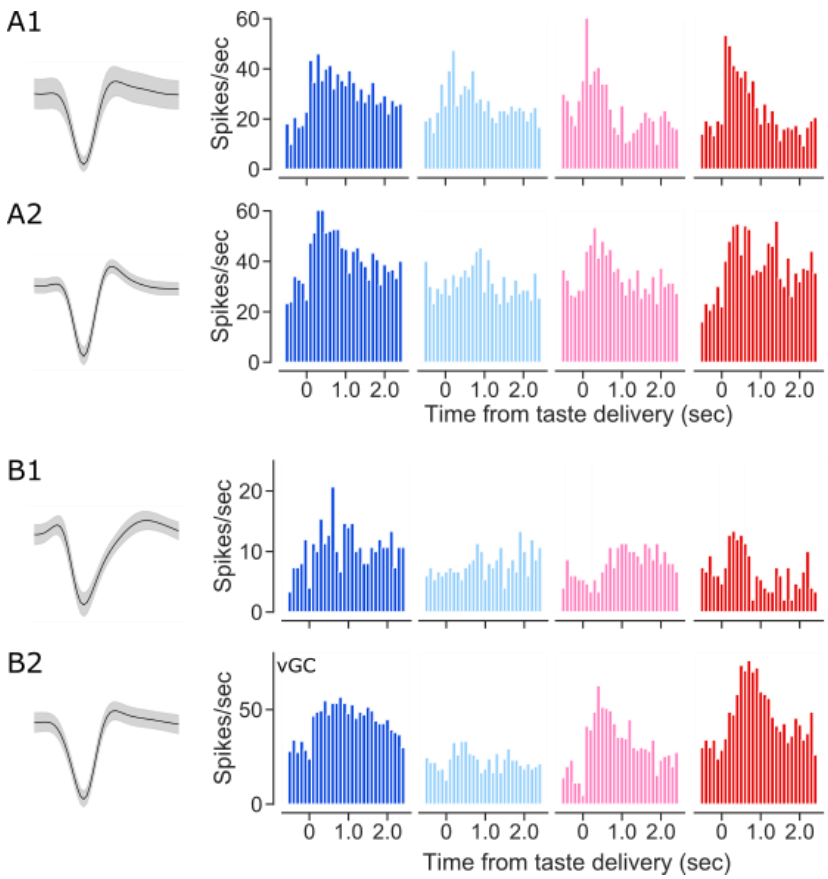


**Figure 7**. **Broadly-responsive ensembles of GC neurons can be recorded from dorsal (A1, A2) and ventral (B1, B2) GC of the same mouse**. **A1-A2**. Representative neurons (wave shapes and PTSHs, conventions as for Figure 2) recorded in dorsal GC. **B1-B2**. Representative neurons recorded from the same mouse in a 2$^{nd}$ session.

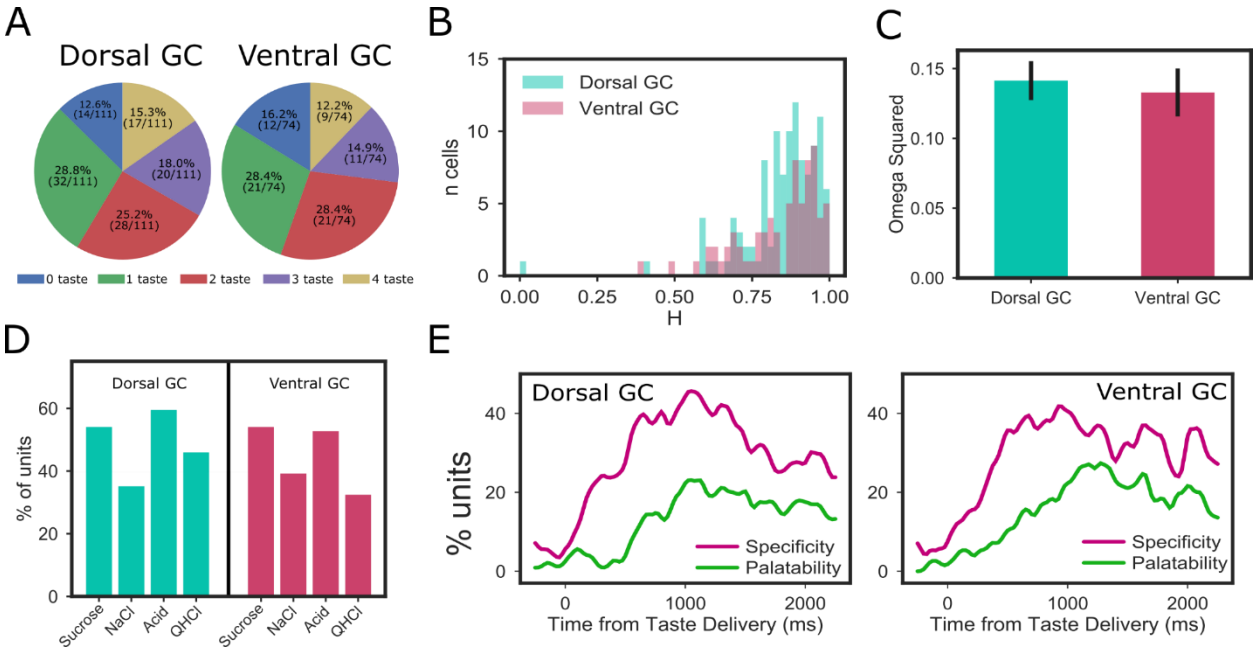


**Figure 8. Dorsal and ventral GC taste responses in mice have similar properties**. **A**. Percentages of dorsal and ventral neurons with significant responses to zero, one, two, three, and four tastes. $X^2$ tests revealed no significant differences between the distributions. **B**. Response entropies (H) for dorsal and ventral GC neurons. A $X^2$ test showed no significant difference between the distributions. **C**. The magnitudes of taste specificity (expressed as omega squared from 2-way ANOVAs, see Methods for details) for dorsal and ventral GC neurons. T-test revealed no difference. **D**. The distribution of relative responsiveness to the four tastes is virtually identical in dorsal and ventral GC—a $X^2$ test did not suggest any differences in which subregion responded to which tastes. **E1-2**. In both dorsal and ventral GC, taste specificity starts to rise immediately after taste delivery and peaks at 500ms, and in both, the emergence and peaking of palatability-related firing was delayed (see Figure 5).

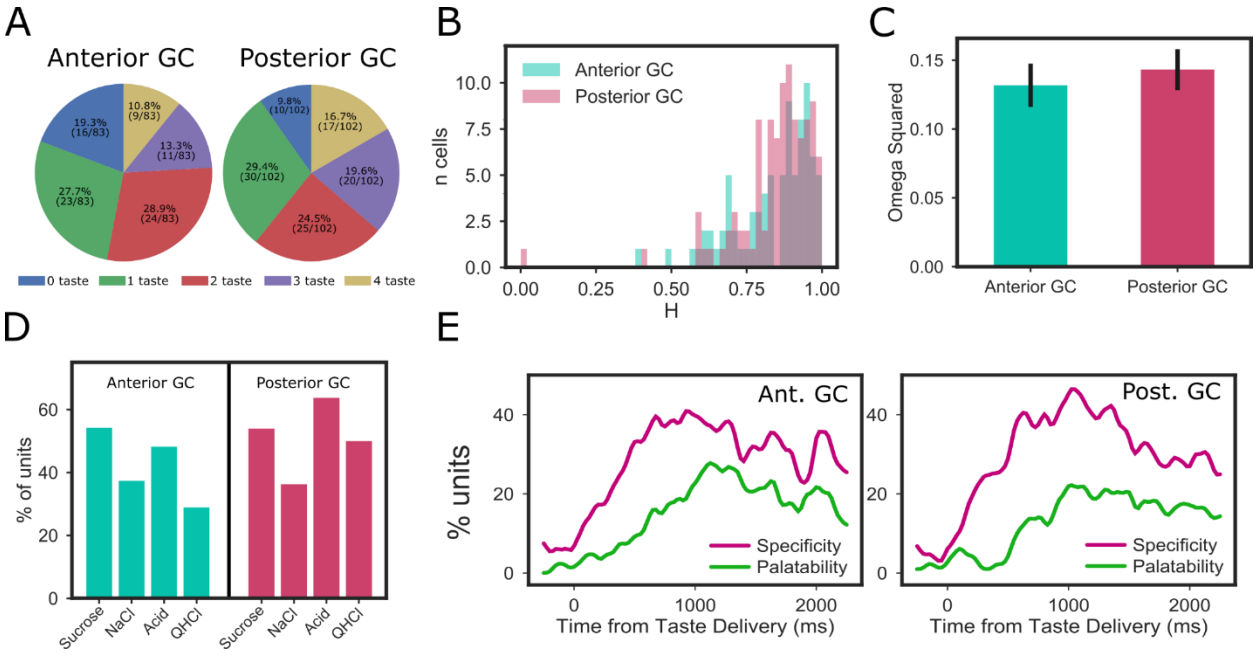


**Figure 9. Anterior and posterior GC taste responses in mice have similar properties**. **A**. Percentages of anterior and posterior neurons with significant responses to zero, one, two, three, and four tastes. $X^2$ tests revealed no significant differences between the distributions. **B**. Response entropies (H) for anterior and posterior GC neurons. A $X^2$ test showed no significant difference between the distributions. **C**. The magnitudes of taste specificity (expressed as omega squared from 2-way ANOVAs, see Methods for details) for anterior and posterior GC neurons. T-test revealed no difference. **D**. The distribution of relative responsiveness to the four tastes in posterior GC was similar to that in anterior GC; while responsiveness to the two more aversive tastes was somewhat higher in posterior GC, a $X^2$ test did not reveal any significant differences in which subregion responded to which tastes. **E1-2**. In both anterior and posterior GC, taste specificity starts to rise immediately after taste delivery and peaks at 500ms, and in both, the emergence and peaking of palatability-related firing was delayed (see Figure 5).